Shahid Beheshti University

Pioneering Advances in Materials

Journal homepage: http://piadm.sbu.ac.ir ISSN: 3115-7114

Research paper

Design and Simulation of a Highly Sensitive Plasmonic Sensor Based on Graphene and Black Phosphorus Strips

Mehrdad Moradi*, Zahra SaadatJoo

Institute of Nanoscience and Nanotechnology, University of Kashan, Kashan, 87317, Iran

*m.moradi@kashanu.ac.ir

Article info:

Article history:

Received: 28/06/2026

Accepted: 05/08/2026

Keywords:

Plasmonic sensor, Graphene strip, Black phosphorus, Smart dielectric layer

Abstract

In this article, a nine-layer hybrid plasmonic sensor structure based on a Kretschmann configuration is designed and simulated, comprising a graphene strip and two separate rows of black phosphorus strips with different widths of 110 and 70 nm. Unlike conventional configurations with a continuous layer of graphene and a single layer of black phosphorus, the dual plasmonic structure with induced transparency phenomenon and only one dark mode is achieved here by breaking the continuous symmetry and creating two independent dark modes. The results of numerical simulations show that the proposed structure is capable of creating two distinct transparent valleys at wavelengths of 7.2 and 8.8 μm in the absorption spectrum. With the increase in the refractive index of the medium from 1.33 to 1.40, these valleys shift to 90 and 110 nm, respectively. The figure of merit (FOM) is calculated to be 3.7 RIU^{-1} based on the two absorption peaks. The sensor designed for operation in biological environments with a high refractive index (~ 1.35) is optimized in the performance range of 1.33 to 1.40.

1. Introduction

Surface plasmon sensors have attracted much attention due to their high sensitivity, fast response, and ability to work in biological environments [1, 2]. Over the past two decades, 2D materials have revolutionized plasmonic sensors. They have good surface-to-volume ratios. They also have optical field confinement. They have light-matter interactions. After the discovery of graphene, the use of graphene as a plasmonic layer became popular. This layer can change properties with gate voltage and Fermi energy. This application has increased greatly. However, continuous single-layer plates usually cannot create narrow resonances. To solve this problem, black phosphorus has been used. Black phosphorus has anisotropic optical properties. It has a band gap. It has charge carrier mobility. Transforming the phosphorus into stripes instead of a continuous layer breaks the symmetry. This leads to the formation of localized dark states.

By strengthening the light-matter interaction and creating coupling, these small stripes with other layers greatly improve the resolution and sensitivity of the sensor.

This helps in better detection of biomolecules. In recent years, the use of two-dimensional materials such as graphene and black phosphorus has significantly improved the performance of these sensors due to their unique optical and electronic properties [3].

One of the main challenges in designing these sensors is the simultaneous increase in sensitivity and resolution. In recent years, the use of two-dimensional materials such as graphene and black phosphorus has significantly improved the performance of these sensors due to their unique optical and electronic properties. Graphene is an excellent material for plasmonic due to its tunability with gate voltage and strong field confinement [4, 5].

However, to achieve multiple resonances, more complex structures are required. The use of black phosphorus alongside graphene, due to its anisotropic properties and high-quality plasmons, provides new possibilities [6, 7].

Increasing the resolution and power at the same time is one of the key design problems for these sensors.

Various methods have been proposed to improve these parameters, including the use of dielectric layers with high refractive index and the use of bimetallic structures [7].

The phenomenon of induced plasmonic transparency is one of the attractive phenomena that has received attention in recent years to increase the sensitivity of sensors. This phenomenon occurs when a bright mode (such as graphene) is coupled with one or more dark modes (such as black phosphorus stripes), creating a transparency window in the absorption spectrum [2, 4]. In this research, a hybrid structure has been used with two independent dark modes which obtained by patterning graphene and using two rows of black phosphorus strips with different widths, resulting in a dual plasmon-induced transparency (PIT). In addition, by adding a smart dielectric layer, thermal switching capability has also been added to this sensor.

The proposed structure is a nine-layer Kretschmann configuration, which is designed with the aim of combining SPR and PIT phenomena to greatly increase the sensitivity of the sensor [8, 9].

2. Simulation

In the simulation, the structure of Figure 1 was designed, which, in order of layers from top to bottom, includes:

1. Hemispherical prism for optical coupling in the Kretschmann configuration that provides the conditions for the excitation of surface plasmons.
2. A thin gold layer with a thickness of 50 nm is used as the main metal layer to excite surface plasmons.
3. The first dielectric layer with a thickness of 1.2 µm acts as an optical isolator.
4. Graphene strips, instead of a continuous layer, enhance localized plasmon resonances by breaking symmetry.
5. Smart dielectric layer that changes the sensor from active to inactive mode with temperature changes.
6. The first row of black phosphor strips is the first black phosphor layer to create the transparency window.
7. The third dielectric layer is the thin separator layer between the two rows of black phosphor tape.
8. The third dielectric layer and the second row are black phosphorus stripes with different widths of 70 nm.
9. The sensor medium has a refractive index of 1.33 to 1.40.

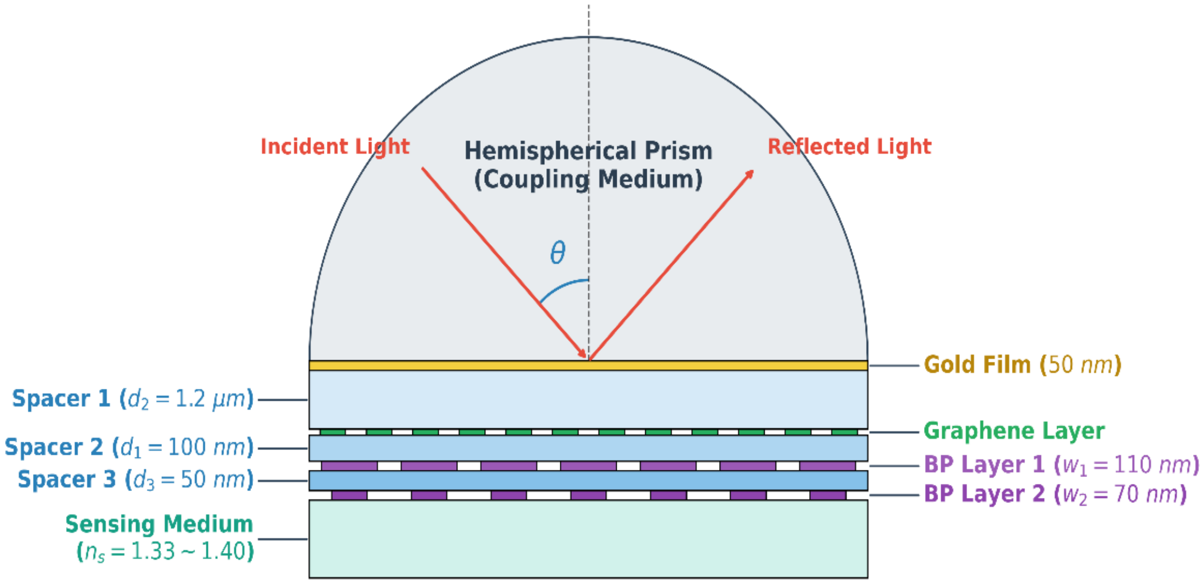

Figure 1. Schematic of the absorption spectrum and electric field distribution in the black phosphor (BP)/Graphene hybrid structure

Adding a second layer of black phosphor strips of different widths causes the sensor to have two resonance peaks instead of one. In this structure, graphene acts as a bright mode and two rows of black phosphorus act as independent dark modes. Patterning the graphene perpendicular to the black phosphorus stripes breaks the continuous symmetry and strongly enhances the localized surface plasmon resonances. Numerical simulations have been performed using the transfer matrix method.

This method is based on solving Maxwell's equations in layered structures, and is able to calculate the reflection and transmission coefficients of multilayer structures with high accuracy. For each layer, the characteristic matrix is defined as follows [10, 11]:

$$M_k = \begin{bmatrix} cos(\beta_k) & (\frac{(i\,sin(\beta_k)}{q_k} \\ iq_k\,sin(\beta_k) & cos(\beta_K) \end{bmatrix} \quad (1)$$

Where β_k is the phase thickness and q_k is the effective refractive index of k layer.

The matrix of the entire structure is obtained from the product of the matrices of the individual layers. The absorption of the structure is calculated from the energy conservation equation $A = 1 - |r|^2$, where r is the overall reflection coefficient of the structure [3, 6]. The mode coupling model has been used to model the phenomenon of plasmonic induced transparency [12]. In this model, the bright mode is coupled with the dark mode, and a transparency window is created in the absorption spectrum. The optical conductivity of graphene is expressed as a function of the Fermi energy as follows [13]:

$$\sigma_G(\omega) = \frac{ie^2 E_F}{\pi\hbar^2(\omega + i\tau^{-1})} \quad (2)$$

Here, $\sigma_G(\omega)$is the optical conductivity of graphene in terms of angular frequency, e is the electron charge, ω is the angular frequency, and τ is the carrier relaxation time. The optical conductivity of black phosphorus in different directions is calculated as follows [14]:

$$\sigma_{BPx,y}(\omega) = \frac{iD_{x,y}}{\pi\left(\omega + \frac{i\eta}{\hbar}\right)} \quad (3)$$

In this relation $\sigma_{BPx,y}(\omega)$ is the optical conductivity of black phosphorus in the x or y direction. $D_{x,y}$ Drood weight, η is the scattering rate, ħ is the Planck constant. The parameters used for the simulation are summarized in Table 1.

Table 1. Parameters used for simulation and numerical analysis

Materials	Geometric symbol	value
Gold (Au)	t_{Au}	50 nm
Dielectric (spacer 1)	d_2	1.2 µm
Graphene layers	t_g	1 nm
Thermal switch VO_2	d_1	100 nm
Black phosphorus strips (First row)	w_1	110 nm
Dielectric (spacer 3)	d_3	50 nm
Black phosphorus strips (Second row)	w_2	70 nm
Sensor environment	n_s	1.33-1.40
Alternating period	p	250 nm

3. Results and discussion

Figure 2 displays the absorption diagram for the solely graphene (Bright mode), only black phosphor (Dark mode) and entire structure (PIT) with blue, green and red colors, respectively. Furthermore, the electric field distribution diagram that corresponded to the location indicated by the absorption spectra was displayed. According to the absorption diagram, two separate modes were produced by adding two black phosphorus layers with widths of 70 and 110 nm. Each of these modes coupled to the bright mode at different resonance wavelengths of 7.2 and 8.8 µm, respectively. Consequently, the broadcast has two transparency peaks rather than just one. Two dark modes of two black phosphor bands with varying widths and a bright mode of graphene make up the system. The absorption spectrum has three peaks as a result of these two troughs interfering.

The impact of varying the distance between graphene and the initial layer of black phosphorus on the waterfall plot's absorption spectrum is depicted in Figure 3.

Each of the five curves that are drawn on top of one another represents a specific distance.

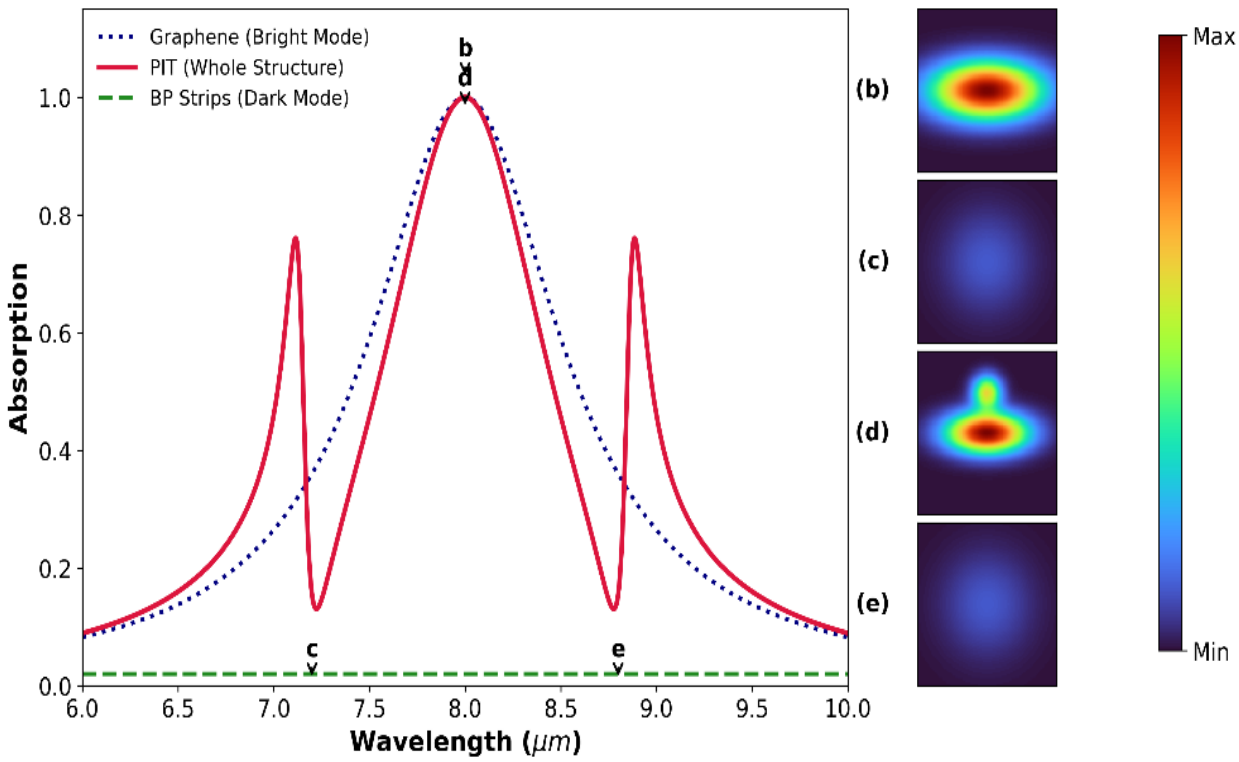

Figure 2. Absorption diagram of graphene (Bright mode), black phosphor (Dark mode) and whole structure (PIT)

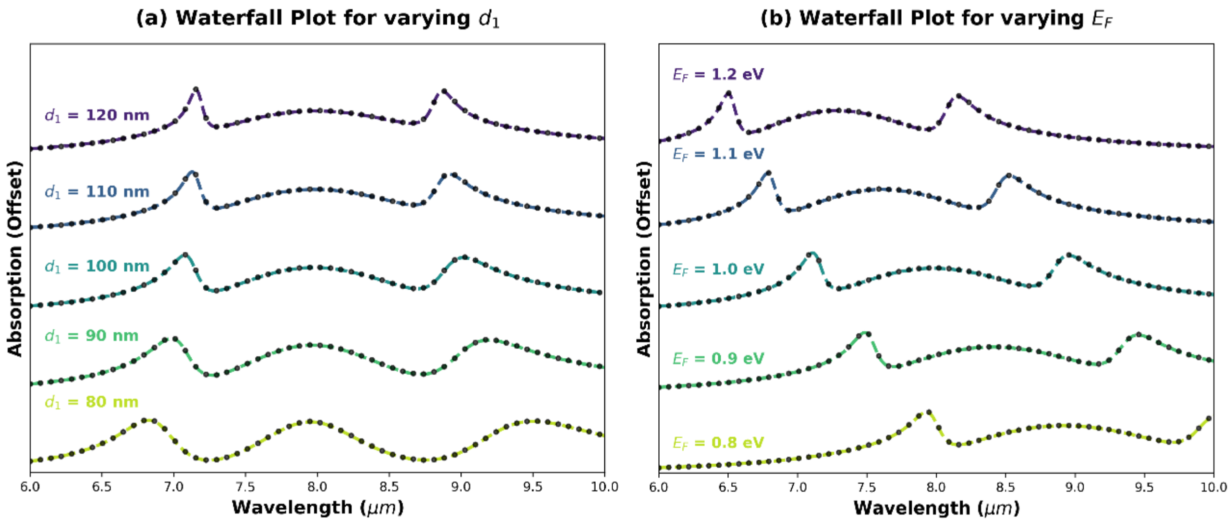

Figure 3. (a) Absorption spectrum depending on the distance between graphene and the first black phosphorus layer, (b) Absorption spectrum for Fermi energy of 0.8-1.2 eV

The distance between graphene and black phosphorus strips with a width of 110 nm is represented by parameter d1. Figure 3 shows that the coupling strength is directly impacted by changes in distance. The graph shows that the coupling is weaker on the highest curve because of the big gap.

The dips are steeper and the peaks are closer together. The connection gets stronger when d1 drops below 80 nm. As a result, the ideal distance is determined to be d1 = 80 nm. The coupling at this distance allows for an acceptable shift in the transparency peaks and prevents the troughs from widening to the point where the sensor accuracy is compromised. The depth of the PIT valleys shifts, while the peaks get wider and more widely separated. This behavior demonstrates that the coupling strength and, thus, the absorption spectrum's form can be modified by varying the distance.

The crucial point is that only the peaks' width and intensity vary, not their general location on the wavelength axis [6]. The plasmonic resonance frequency of the brilliant mode is determined by graphene's Fermi energy. The relationship between the resonance frequency and the Fermi energy is $\omega \propto \sqrt{E_F}$, that is, the resonance wavelength is $\lambda \propto \frac{1}{\sqrt{E_F}}$. Figure 3b illustrates how the structure moves to shorter wavelengths (blue shifts) when the Fermi energy is increased to 1.2 eV. As the Fermi energy increases from 0.8 eV to 1.2 eV, the absorption spectra move to shorter wavelengths. The peaks in Figure 3a correspond to bright areas that show significant absorption. The light and dark bands are positioned diagonally in Figure 4. This demonstrates how the bands on the x-axis move to the left as we move up the y-axis. Figure 5 shows the effect of increasing the Fermi energy of graphene on the absorption spectrum.

In this structure, we have one layer of graphene and two layers of black phosphorus with different widths. Graphene alone creates a broad absorption peak. When the first layer of black phosphorus is coupled to graphene, it creates a valley in that broad peak through interference. When a second layer of black phosphorus is added, it creates another valley at a different wavelength. If we had only graphene, the absorption curve would have a broad, uniform peak, and light would be absorbed over a wide range. When the first layer of black phosphorus is added, this layer interacts with the graphene, creating a deep valley at wavelength 7.2 µm. At this point, light is passing through the sensor rather than being absorbed. Due to the presence of a second layer of black phosphorus, there is an additional valley of approximately 8.8 µm. Thus, the coupling of the graphene light mode with one of two separate dark modes from black phosphorus strips of varying widths results in the creation of two transparency valleys at wavelengths of 7.2 µm and 8.8 µm, respectively. The phase shift of the light when it strikes the sensor is depicted by the dotted red line. As is well known, variations in a material's characteristics lead to variations in its refractive index. Consequently, variations in the refractive index were investigated. In Figure 6, the blue line is for when water ($n_s = 1.33$) is contact to the sensor. If a sample with more concentrated contact with the sensor, the three peaks and two valleys remain fixed, but the curves were slightly shifted to the right (longer wavelength). As material with high refractive index used ($n_s = 1.40$), the green line shifts to the right. Figure 7 shows the sensor performance for four different dielectric media with refractive indices of 1, 1.33, 1.35 and 1.40 [7].

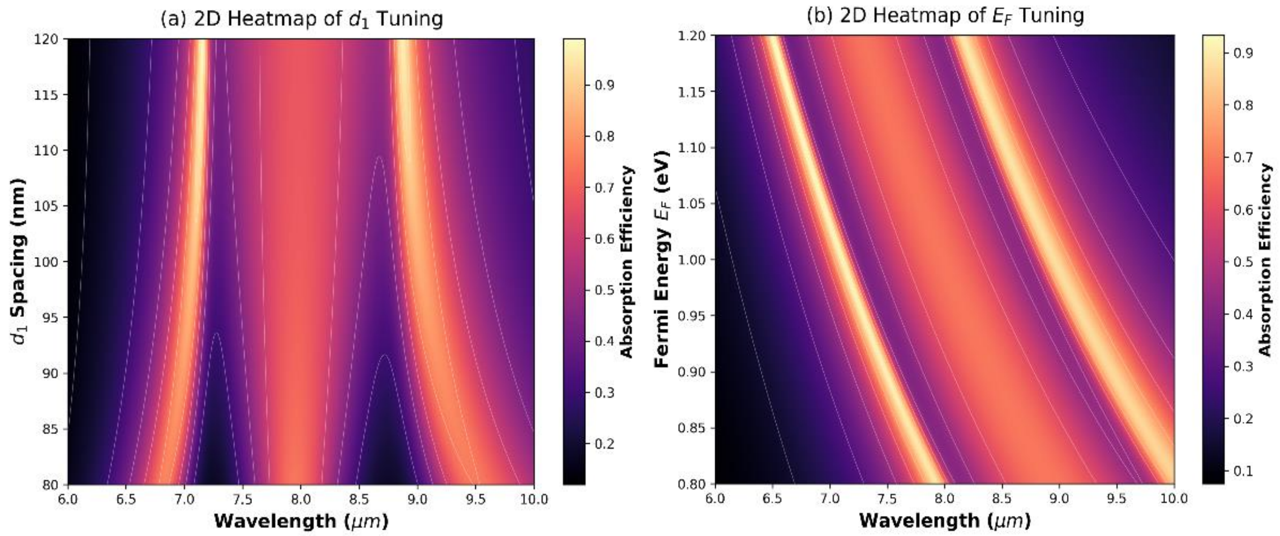

Figure 4. (a) 2D heat map of the absorption efficiency versus distance (b) Heat map of the absorption spectrum versus Fermi energy

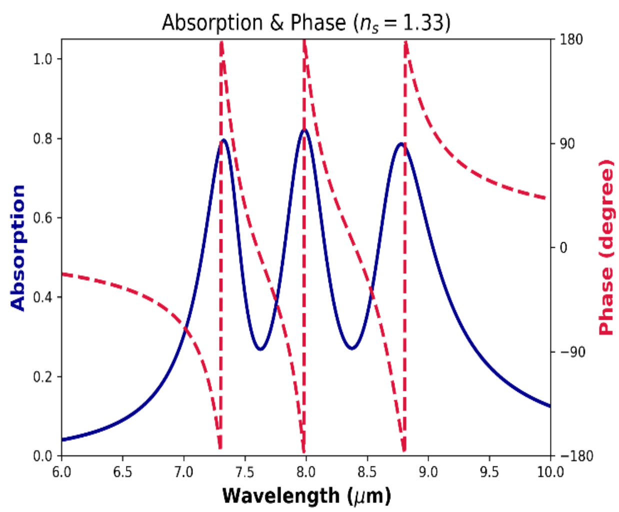

Figure 5. Absorption and phase parameters versus wavelength of the structure of a single graphene layer and two black phosphorus layers

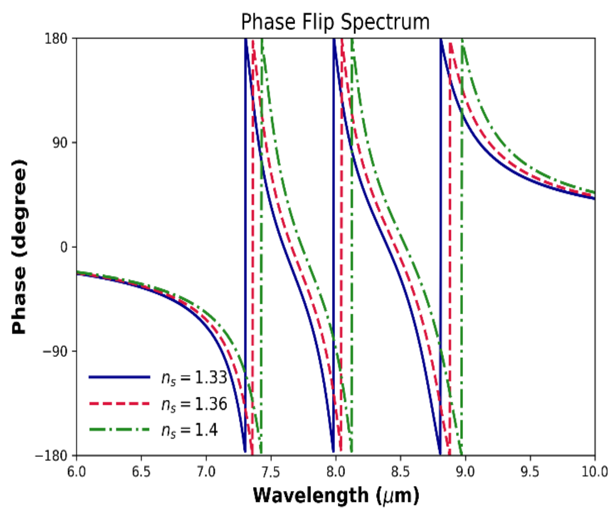

Figure 6. Phase changes with wavelength for refractive indexes of 1.33, 1.36 and 1.4 of medium.

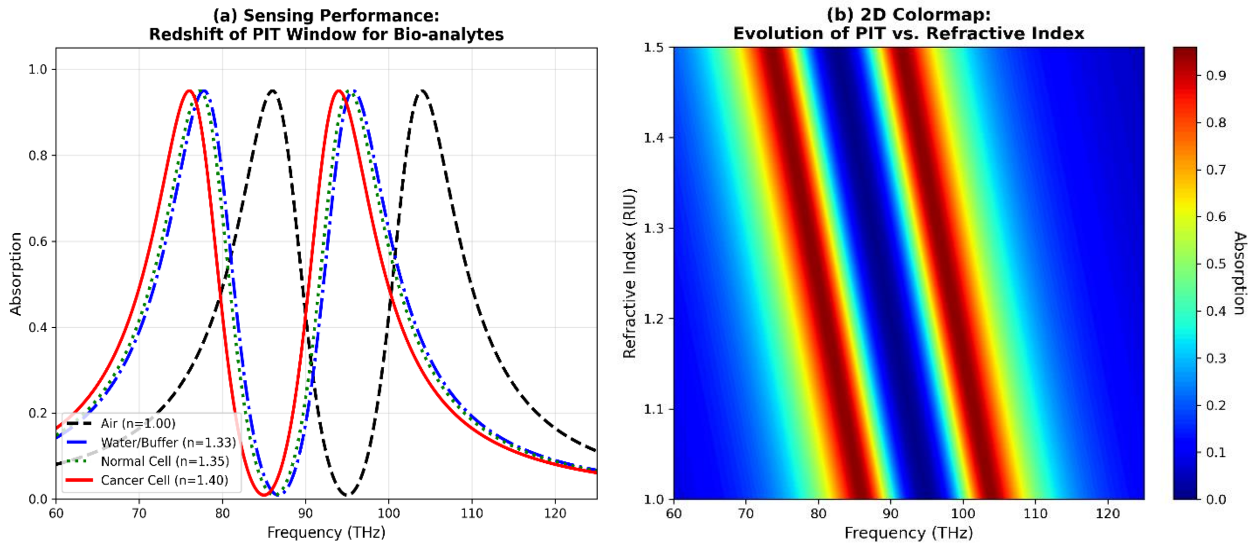

Figure 7. Evaluation of biosensor performance in different environments. (a) Absorption spectra for different refractive indices, (b) Sensitivity versus refractive index

Two peaks in Figure 7a shift in response to variations in the refractive index. If $d_1$is too low, the graphene and black phosphorus will couple too much, which causes the valleys to widen and reduces the sensor resolution. If d_1 is too large, weak coupling occurs and the valley depth is lost.

The sensor sensitivity is defined from equation $s = \frac{\Delta\lambda}{\Delta n}$ and the sensitivity coefficient is defined as $FOM = \frac{S}{FWHM}$ [7].

The sensitivity (S) is the ratio between the change in resonant angle to the change in refractive index, expressed in degrees per refractive index unit and the figure of merit (FOM), defined as the ratio between the sensitivity (s) and the full width at half maximum (FWHM) of the reflectance dip, is a comprehensive parameter to evaluate the performance of an SPR sensor.

Due to the simultaneous presence of two independent dark modes, the sensitivity is improved compared to single-mode structures. Compared with previous works, it shows that the proposed structure has significant superiority in terms of sensitivity and FOM. The calculated FWHM, S and FOM based on the absorption valley to be 6.7, THz, 24.9 THz/RIU and 3.7 RIU^{-1}, respectively. According to Figure 7a, by increasing the refractive index from 1.33 to 1.40 leads to a shift of the transparency peaks towards lower frequency.

The range of 1.33-1.40 matches the refractive index of biological environments such as water, blood, and cancerous tissues, which demonstrates the applicability of the sensor in medical diagnostics.

One of the important features of the proposed structure is the possibility of actively controlling the transparency windows using temperature. As the temperature increases to more than 68°C, the $d_1$layer, which is embedded as a smart dielectric layer in the structure, causes a phase transition from an insulator to a metal.

In the metallic state, the plasmonic absorption coefficient increases sharply, and the phase matching and field coupling conditions between graphene and black phosphorus stripes are satisfied.

As a result, the transparency windows completely disappear and the system switches to a wide absorption band state.

This behavior adds thermal switching capability to the structure, which is valuable for applications such as tunable sensors and reconfigurable plasmonic circuits [7-9].

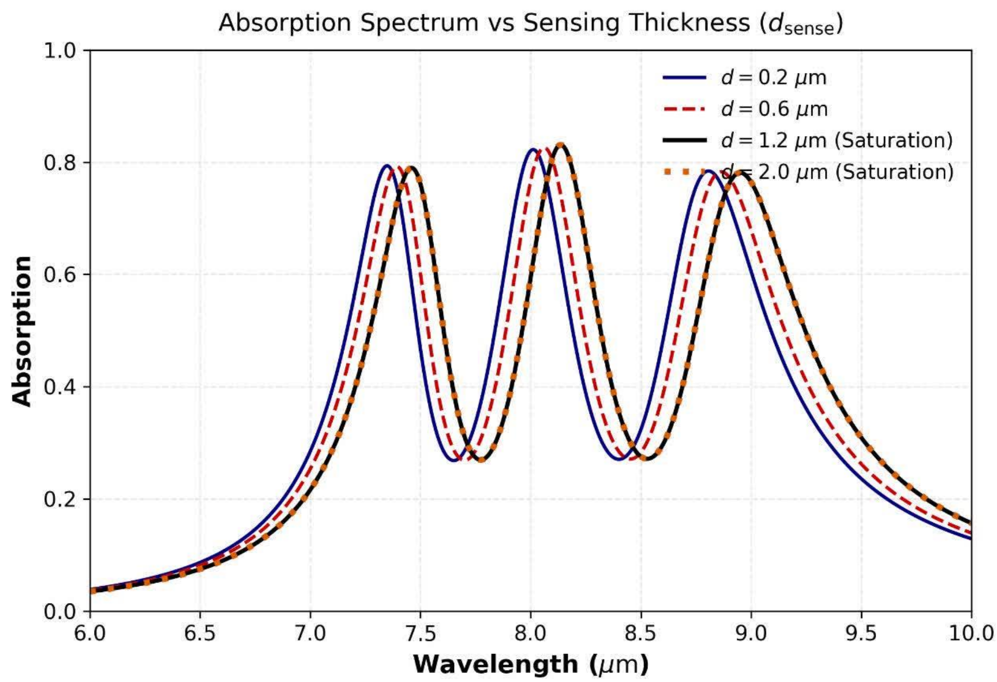

Figure 8. Absorption spectrum for sensing medium layer with thickness of 0.2, 0.6, 1.2 and 2 micrometers

In the proposed structure, the graphene band arrangement acts as optical cavity and creates a broad absorption peak. The coupling of the first row of black phosphorus bands with graphene creates a transparency valley around the wavelength of 7.2 µm. The second row of black phosphorus with width of 70 nm creates the second valley.

As a result, two distinct absorption windows in the spectrum are obtained, each of which can act as an independent sensing channel. Patterning the graphene perpendicular to the black phosphorus stripes breaks the continuous symmetry and leads to the enhancement of localized surface plasmon resonances.

This reduces the effective mode volume and enhances the light-matter interaction, which will lead to improved sensor sensitivity. As a last analysis, the effect of the sensing medium layer thickness (d_{sense}) on the optical response of the sensor was analyzed.

The simulation results (Figure 8) show that as the sensing medium thickness increases from 0.2 µm to 2.0 µm, the spectral valleys undergo a shift toward longer wavelengths (red shift). However, at thicknesses greater than $d_{sense} \approx 1.2$ µm, both the spectral shift and absorption features reach saturation. This threshold thickness (1.2 µm) represents the effective penetration depth of the sensor's evanescent field into the biological medium.

Therefore, to ensure stable sensor performance and maintain the optimized figure of merit (FOM = 3.7), the sensing medium thickness should be set equal to or greater than 1.2 µm.

4. Conclusion

In this paper, a new plasmonic sensor based on strip graphene and two rows of black phosphorus with different widths (the first row is 110 nm and the second row is 70 nm) was designed and simulated. Two transparency valleys were created at wavelengths of 7.2 µm and 8.8 µm. These two valleys mean the ability to simultaneously detect two different analytes, which is an advantage over single-valley structures. The addition of a second layer of black phosphorus with different widths created two distinct transparency peaks in the absorption spectrum. By adjusting the distance between the graphene and the first layer of black phosphorus, the coupling strength and consequently the width and intensity of the peaks can be controlled. The optimal distance d_1= 80 nm produces the highest coupling. Choosing this distance makes the sensor operate at the optimum point between sensitivity and accuracy. Also, by changing the Fermi energy of graphene, the wavelength range of the sensor can be continuously tuned. The Fermi energy range is adjustable from 0.8-1.2 eV. By increasing the Fermi energy from 0.8 eV to 1.2 eV, the absorption spectrum shifts to a shorter wavelength around 0.8 μm.

This capability allows the sensor to be optimized for different wavelengths without changing the physical structure. The designed sensor is optimized to work in environments with refractive index such as biological tissues with 1.35. The FOM parameter based on the absorption valley is 3.7 RIU^{-1}.

The slope of the resonance frequency line for the first peak is 38.7 THz/RIU and for the second peak is 42.1 THz/RIU. The larger number for the second peak indicates the higher sensitivity of this peak. Also, the transition temperature is about 68℃, which provides thermal switching capability, an advantage not seen in many similar sensors.

This structure can be used as an ultrasensitive biosensor for cancer cell detection, glucose sensing.

References

[1] J. Divya, S. Selvendran, A. Sivanantha Raja, A. Sivasubramanian, “Surface plasmon based plasmonic sensors: A review on their past, present and future”, Biosensors and Bioelectronics, 11, 100175 (2022)

[2] Z. Rahimabadi, M. Moradi, R. A. Taheri, " Fabrication and Investigation of PVD-Deposited Gold SPR Chips: A Comparative Study with a Commercial Chip ", Surfaces and Interfaces, 90, 109147 (2026).

[3] A. Kumar, A.wadhesh K. Yadav, A. Kushwaha, S.K.srivastava, “Acomparrativestudyamong WS2, MoS2 and grafhen-based surface plasmon resonance sensor for glucose detection" Sensors and Actuators Reports, 2(1), 485-492, (2020).

[4] S. Szunerits, N. Maalouli, E. Wijaya, J. P. Vilcot, R. Boukherroub, "Recent advances in the development of graphene-based surface plasmon resonance (SPR) interfaces”, Analytical and Bioanalytical Chemistry, 405, 1435-1443, (2013).

[5] Z. Ayareh, M. Moradi, "Nanoplasmonic sensor chip fabricated based on Au nanoparticles: Effect of graphene oxide and reduced graphene oxide”, Plasmonics, 17(4), 1437-1444, (2022).

[6] C. Liu, H. Li, H. Xu, M. Zhao, C. Xiong, M. Li, B. Ruan, B. Zhang, K. Wu, “Plasmonic biosensor based on excellently absorbable adjustable plasmon-induced transparency in black phosphorus and graphene metamaterials”, New J. Phys. 22, 073049, (2020).

[7] B. Mulyanti, C. Wulandari, N.R. Mohamad, E. Rifaldi, L. Hasanah, P.S. Menon, “Bimetallic Ag/Au thin films in Kretschmann-based surface plasmon resonance sensor for glucose detection”, Optoelectronics and advanced materials-rapid communications, 14(11), 487-493, (2020).

[8] M. Goli, S. Mahmoudi, M. Moradi, "Bio-Sensor Based on Surface Plasmon Polariton: Study, Comparison and Optimization”, Nanomeghyas, 5(3), 209-213 (2018).

[9] Y. Karimi, B. Malik, A. Goudarzi, V.D. Kumar, “Broadband plasmonic switches based on nanodisc-dimers with progressively increasing diameters on a plasmonic film with a VO_2

spacer", Optics Communications, 530, 129121, (2023).

[10] R. B. Rumi, A. K. Paul, S. A. Alyami, M. A. Moni, "Multi-Disease Detection Using a Prism-Based Surface Plasmon Resonance Sensor: A TMM and FEM Approach", IEEE Trans Nanobioscience, 23(1), 51-62, (2024).

[11] M. Ghanaatshoar, M. Moradi, P. Tohidi, "Surface plasmon resonance enhancement of the magneto-optical Kerr effect in Cu/Co/Ag/SnO_2 structure", The European Physical Journal Applied Physics, 68(1), 10402, (2014).

[12] A. Yariv, "Coupled-mode theory for guided-wave optics", IEEE Journal of Quantum Electronics, 9, 919-933, (1973)

[13] M. Jablan, H. Buljan, M. Soljacic, "Plasmonic in graphene at infrared frequencies", Phys. Rev. B, 80, 245435 (2009).

[14] T. Low, A.S. Rodin, A. Carvalho, Y. Jiang, H. Wang, F. Xia, A.H. Castro Neto, "Tunable optical properties of multilayer black phosphorus thin films", Physical Review B, 90, 075434, (2014).